Chapter 1

Tau Decays into Hadrons

The τ lepton is an elementary particle with spin $1/2$ and a mass of $1.776\,86\,\mathrm{GeV}$ [**PDG2018**]. It is the only lepton heavy enough to decay into hadrons but also light enough for performing a low-energy QCD analysis. Its inclusive hadronic[1] decay ratio is given by

$$R_\tau = \frac{\Gamma(\tau \to \nu_\tau + \text{hadrons})}{\Gamma(\tau \to \nu_\tau e^- \overline{\nu_e})} \tag{1.0.1}$$

and sensible to the strong coupling, due to its rather large value, at the m_τ^2 scale, of approximately 0.33. On the other hand $\alpha_s(m_\tau^2)$ is small enough to apply the OPE. The NP OPE contributions to the decay ratio are suppressed. The dimension two contribution of the OPE is proportional to the quark masses and has only a tiny contribution for light quarks. The dimension four contribution can be suppressed by applying weight functions, that do not have a monomial in x. E.g. the kinematic weight $\omega_\tau = (1-x)^2(1+2x) = 1-3x^2+2x^3$ is not sensitive to OPE corrections of dimension four. The dimension six contribution of the OPE is proportional to $1/(m_\tau^2)^3$ and further suppressed in the V+A channel of the vector and axial-vector $D = 6$ contributions have opposite signs and partly cancel themselves. Higher dimensional OPE contributions are suppressed by terms $1/m_\tau^n$ with $n \geqslant 8$. As a result the perturbative contributions are dominant. They are known up to order $\mathcal{O}(\alpha_s^4)$ with a total contribution of 20% to R_τ [**Pich2016a**], which enables us to perform precise calculations of the inclusive τ decay ratio. Furthermore by extracting α_s at low energies at the

[1] Meaning all decay channels with a hadron in its final state.

scale of m_τ^2 we will achieve lower errors for the strong coupling at higher energies as the errors run with the strong coupling and get smaller with increasing energy.

The τ decays permit one of the most precise determinations of the strong coupling α_s. Building on the previously presented QCDSR we will now elaborate the needed theory to extract α_s from the process of hadronic τ decays.

1.1 The Inclusive τ Decay Ratio

The theoretical expression of the inclusive hadronic τ decay ratio (eq. 1.0.1) is given by

$$R_\tau(s) = 12\pi S_{EW}|V_{ud}|^2 \int_0^{m_\tau} \frac{ds}{m_\tau^2}\left(1-\frac{s}{m_\tau^2}\right)\left[\left(1+2\frac{s}{m_\tau^2}\right)\operatorname{Im}\Pi^{(1)}(s)+\operatorname{Im}\Pi^{(0)}(s)\right], \tag{1.1.1}$$

where S_{EW} is the electroweak correction, V_{ud} the corresponding *Cabibbo-Kobayashi-Maskawa* (CKM) matrix element and $\operatorname{Im}\Pi$ the imaginary part of the two-point function. For brevity we will omit the electroweak S_{EW} and CKM factors from now on. Equation 1.1.1 was first derived in [**Tsai1971**], using current algebra, a more recent derivation making use of the *optical theorem* can be taken from [**Schwab2002**]. Notice that we used the standard Lorentz decomposition into transversal ($J=1$) and longitudinal ($J=0$) components of **??** to display the hadronic decay ratio (eq. 1.1.1).

Applying Cauchy's theorem, as seen in **??**, to the eq. 1.1.1 we can rewrite the line integral into a closed contour integral

$$R_\tau = 6\pi i \oint_{s=m_\tau} \frac{ds}{m_\tau^2}\left(1-\frac{s}{m_\tau^2}\right)\left[\left(1+2\frac{s}{m_\tau^2}\right)\Pi^{(1)}(s)+\Pi^{(0)}(s)\right]. \tag{1.1.2}$$

It is convenient to work with a slightly different combination of transversal and longitudinal components $\Pi^{(1+0)}$, which has been defined in **??** and is free of kinematic singularities. As a result we can further rewrite the hadronic τ decay ratio into

$$R_\tau = 6\pi i \oint_{|s|=m_\tau} \frac{ds}{m_\tau^2}\left(1-\frac{s}{m_\tau^2}\right)^2\left[\left(1+2\frac{s}{m_\tau^2}\right)\Pi^{(1+0)}(s)-\left(\frac{2s}{m_\tau^2}\right)\Pi^{(0)}(s)\right]. \tag{1.1.3}$$

In the case of τ decays we only have to consider vector and axial-vector contributions of decays into up, down and strange quarks.

With eq. 1.1.3 we have a suitable physical quantity that can be theoretically calculated as experimentally measured. By using the QCDSR we apply a closed contour integral of radius s_0. As a result we successfully avoid low energies at which the application of PT would be questionable. For example if we would choose a radius with the size of the τ mass $m_\tau \approx 1.78\,MeV$ the strong coupling would have a perturbatively safe value of $\alpha_s(m_\tau^2) \approx 0.33$ [**Pich2016**]. Obviously we would benefit even more from a contour integral over a bigger circumference, but τ decays are kinematically limited by their mass. Nevertheless there are promising e^+e^- annihilation data, which yield valuable inclusive decay ratio values up to $2\,GeV$ [**Boito2018**][**Keshavarzi2018**].

1.1.1 Renormalisation Group Invariance

We have seen in **??**, that the two-point function is not a physical quantity, as the dispersion relation (**??**) contains an unphysical polynom. Luckily for the vector correlator, appearing in hadronic τ decays, the polynom is just a constant. Consequently we can take the derivative with respect to the momentum s to derive a physical quantity from the two-point function:

$$D(s) \equiv -s\frac{d}{ds}\Pi(s). \tag{1.1.4}$$

$D(s)$ is called the *Adler function* and fulfils, as all physical quantities, the RGE (**??**). The Adler function commonly has separate definitions for the longitudinal plus transversal and the solely longitudinal contributions:

$$D^{(1+0)}(s) \equiv -s\frac{d}{ds}\Pi^{(1+0)}(s), \qquad D^{(0)}(s) \equiv \frac{s}{m_\tau^2}\frac{d}{ds}(s\Pi^{(0)}(s)). \tag{1.1.5}$$

The two-point functions in eq. 1.1.3 can now be replaced with the help of partial integration

$$\int_a^b u(x)V(x)\,dx = \big[U(x)V(x)\big]_a^b - \int_a^b U(x)v(x)\,dx. \tag{1.1.6}$$

We will perform two separate computations for the two cases $(1+0)$ and (0).

Starting by the transversal plus longitudinal contribution we get:

$$\begin{aligned} R_\tau^{(1)} &= \frac{6\pi i}{m_\tau^2}\oint_{|s|=m_\tau^2} \underbrace{\left(1-\frac{s}{m_\tau^2}\right)^2\left(1+2\frac{s}{m_\tau^2}\right)}_{=u(x)}\underbrace{\Pi^{(1+0)}(s)}_{=V(x)} \\ &= \frac{6\pi i}{m_\tau^2}\left\{\left[-\frac{m_\tau^2}{2}\left(1-\frac{s}{m_\tau^2}\right)^3\left(1+\frac{s}{m_\tau^2}\right)\Pi^{(1+0)}(s)\right]_{|s|=m_\tau^2}\right. \\ &\quad \left.+\oint_{|s|=m_\tau^2}\underbrace{-\frac{m_\tau^2}{2}\left(1-\frac{s}{m_\tau^2}\right)^3\left(1+\frac{s}{m_\tau^2}\right)}_{=U(x)}\underbrace{\frac{d}{ds}\Pi^{(1+0)}(s)}_{=v(x)}\right\} \\ &= -3\pi i\oint_{|s|=m_\tau^2 s}\frac{ds}{s}\left(1-\frac{s}{m_\tau^2}\right)^3\left(1+\frac{s}{m_\tau^2}\right)\frac{d}{ds}D^{(1+0)}(s) \end{aligned} \tag{1.1.7}$$

where we fixed the integration constant to $c = -\frac{m_\tau^2}{2}$ in the second line and left the antiderivatives contained in the squared brackets untouched. If we parametrise the integral appearing in the expression in the squared brackets we can see that it vanishes:

$$\left[-\frac{m_\tau^2}{2}\left(1-e^{-i\phi}\right)^3\left(1+e^{-i\phi}\right)\Pi^{(L+T)}(m_\tau^2 e^{-i\phi})\right]_0^{2\pi} = 0, \tag{1.1.8}$$

where $s \to m_\tau^2 e^{-i\phi}$ and $(1-e^{-i\cdot 0}) = (1-e^{-i\cdot 2\pi}) = 0$. Repeating the same calculation for the longitudinal part yields

$$\begin{aligned} R_\tau^{(0)} &= \oint_{|s|=m_\tau^2} ds\left(1-\frac{s}{m_\tau^2}\right)^2\left(-\frac{2s}{m_\tau^2}\right)\Pi^{(0)}(s) \\ &= -4\pi i\oint\frac{ds}{s}\left(1-\frac{s}{m_\tau^2}\right)^3 D^{(0)}(s). \end{aligned} \tag{1.1.9}$$

Consequently combining the transversal with the longitudinal contribution results in

$$R_\tau = -\pi i\oint_{|s|=m_\tau^2}\frac{ds}{s}\left(1-\frac{s}{m_\tau^2}\right)^3\left[3\left(1+\frac{s}{m_\tau^2}D^{(1+0)}(s)+4D^{(0)}(s)\right)\right]. \tag{1.1.10}$$

It is convenient to define $x = s/m_\tau^2$ such that we can rewrite the inclusive ratio as

$$R_\tau = -\pi i\oint_{|s|=m_\tau^2}\frac{dx}{x}(1-x)^3\left[3(1+x)D^{(1+0)}(m_\tau^2 x)+4D^{(0)}(m_\tau^2 x)\right], \tag{1.1.11}$$

which will be the final expression we will be using to express the inclusive τ decay ratio.

1.2 Theoretical Computation of R_τ

The previously derived expression for the τ decay ratio is at first approximation equal to the number of colours [**Peskin1995**]

$$R_\tau \approx N_c. \tag{1.2.1}$$

If we take the perturbative δ_{pt} and non-perturbative δ_{npt} contributions into account we can organise the vector and axial-vector inclusive decay ratio as

$$R^{\omega}_{\tau,V/A} = \frac{N_c}{2}\left(1 + \delta^{\omega}_{pt} + \delta^{\omega}_{npt}\right). \tag{1.2.2}$$

Note that the factor $1/2$ comes from the fact, that in the chiral limit the vector and axial-vector contributions are equal. The dependence on the chosen weight function ω is reflected in the upper indices.

For the kinematic weight (**??**), which appears naturally in the tau decay ratio,

$$\omega_\tau \equiv (1-x)^2(1+2x), \tag{1.2.3}$$

we have a dominant perturbative contribution of $\delta_{pt} \approx 20\%$ to R_τ [**Pich2013**] and a minor, but not negligible, non-perturbative contribution of $\delta^{NP}_{V+A} \lesssim 1\%$ [**Jamin2013**] for the $V+A$-channel.

In the following we want to derive the theoretical expressions needed to calculate both of the corrections to eq. 1.2.2 starting with the perturbative one.

1.2.1 The Perturbative Contribution

The perturbative contribution δ_{pt} to the inclusive τ decay ratio is corresponds to the first term of the OPE. Currently the perturbative expansion has been calculated to fourth order $\mathcal{O}(\alpha_s^4)$. Due to their role as dominant corrections their uncertainties from unknown higher-order corrections dictate the final error of the determination of the strong coupling [**Pich2016**].

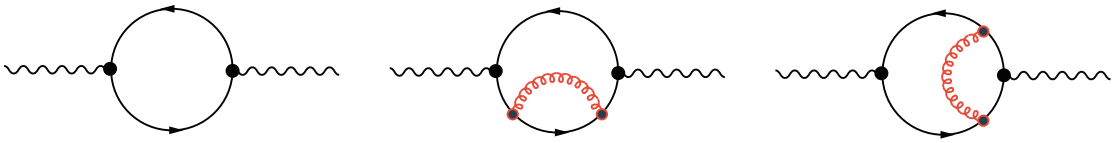

Figure 1.1: Feynman loop diagrams to calculate the $c_{n,k}$ coefficients of the expanded correlator $\Pi_V^{(1+0)}$. The internal red lines represent gluons. Diagram a) represents the parton model and diagrams b) and c) represent higher order corrections.

We will treat the correlator in the chiral limit, in which the scalar and pseudoscalar contribution of the two-point function vanish and the axial and vectorial contributions are equal. As a result we can focus ourselves on the vector correlator $\Pi_V(s)$, which can be expanded as a sum over different orders of α **[Beneke2008]**:

$$\Pi_V^{(1+0)}(s) = -\frac{N_c}{12\pi^2}\sum_{n=0}^{\infty} a_\mu^n \sum_{k=0}^{n+1} c_{n,k} L^k \quad \text{with} \quad L \equiv \ln\frac{-s}{\mu^2}, \tag{1.2.4}$$

where we defined $a_\mu \equiv \alpha(\mu)/\pi$. The coefficient $c_{n,k}$ up to two-loop order can be obtained by Feynman diagram calculations. With the diagrams of fig. 1.1 we can calculate the one-loop result of the correlator **[Jamin2006]**

$$\Pi^B(q^2)\Big|^{1-\text{loop}} = \frac{N_c}{12\pi^2}\left(\frac{1}{\hat{\epsilon}} - \log\frac{(-q^2 - i0)}{\mu^2} + \frac{5}{3} + \mathcal{O}(\epsilon)\right), \tag{1.2.5}$$

where $\Pi^B_{\mu\nu}(q^2)$ is the bare two-point function[2]. This result can then be used to extract the first two coefficients of the correlator expansion given in eq. 1.2.4

$$c_{0,0} = -\frac{5}{3} \qquad \text{and} \qquad c_{0,1} = 1. \tag{1.2.6}$$

The second loop can also be calculated by diagram techniques resulting in **[Boito2011]**

$$\Pi_V^{(1+0)}(s)\Big|^{2-\text{loop}} = -\frac{N_c}{12\pi^2} a_\mu \log(\frac{-s}{\mu^2}) + \cdots \tag{1.2.7}$$

yielding $c_{1,1} = 1$.

[2]The term $1/\hat{\epsilon}$, which is of order zero in α_s, is not present in the Adler function or the imaginary part of the correlator.

Beginning from three loop diagrams the algebra becomes exhausting and one has to use dedicated algorithms to compute the higher loops. The third loop calculations have been done in the late seventies [**Chetyrkin1979**, **Dine1979**, **Celmaster1979**]. The four loop evaluation have been completed a little more than ten years later [**Gorishnii1990**, **Surguladze1990**]. The highest loop published, that amounts to α_s^4, was published in 2008 [**Baikov2008**] almost 20 years later.

Fixing the number of colours to $N_c = 3$ the missing coefficients up to order four in α_s read:

$$\begin{aligned} c_{2,1} &= \frac{365}{24} - 11\zeta_3 - \left(\frac{11}{12} - \frac{2}{3}\zeta_3\right) N_f \\ c_{3,1} &= \frac{87029}{288} - \frac{1103}{4}\zeta_3 + \frac{275}{6}\zeta_5 \\ &\quad - \left(\frac{7847}{216} - \frac{262}{9}\zeta_3 + \frac{25}{9}\zeta_5\right) N_f + \left(\frac{151}{162} - \frac{19}{27}\zeta_3\right) N_f^2 \\ c_{4,1} &= \frac{78631453}{20736} - \frac{1704247}{432}\zeta_3 + \frac{4185}{8}\zeta_3^2 + \frac{34165}{96}\zeta_5 - \frac{1995}{16}\zeta_7, \end{aligned} \tag{1.2.8}$$

where used the flavor number $N_f = 3$ for the last line.

The 6-loop calculation has until today not been computed, but Beneke and Jamin [**Beneke2008**] used and educated guess to estimate the coefficient

$$c_{5,1} \approx 283 \pm 283. \tag{1.2.9}$$

We often see $c_{5,1}$ applied to estimate the perturbative errors related to missing higher order contributions.

In stating the coefficients $c_{n,k}$ of the correlator expansion we have restricted ourselves to k indices equal to one. This is due to the RGE, which relates coefficients with k different than one to coefficients with k equal to one ($c_{n,1}$). Consequently the correlator $\Pi_V^{1+0}(s)$ needs to be a physical quantity, which we can be achieved with the previously defined Adler function (eq. 1.1.5). The correct expression for the correlator expansion in eq. 1.2.4 is then given by

$$D_V^{(1+0)} = -s\frac{d\Pi_V^{(1+0)}(s)}{ds} = \frac{N_c}{12\pi^2}\sum_{n=0}^{\infty} a_\mu^n \sum_{k=1}^{n+1} k c_{n,k} L^{k-1}, \tag{1.2.10}$$

where we used $dL^k/ds = k\ln(-s/\mu^2)^{k-1}(-1/\mu^2)$. Applying the RGE (**??**) to the

scale-invariant Adler function yields

$$-\mu\frac{d}{d\mu}D_V^{(1+0)} = -\mu\frac{d}{d\mu}\left(\frac{\partial}{\partial L}\,dL + \frac{\partial}{\partial a_s}\,da_s\right)D_V^{(1+0)} = \left(2\frac{\partial}{\partial L} + \beta\frac{\partial}{\partial a_s}\right)D_V^{(1+0)} = 0, \tag{1.2.11}$$

where we made use of the β-function, which is defined in **??**, and of the expression $dL/\,d\mu = -2/\mu$.

The relation between the correlator expansion coefficients can then be taken by calculating the Adler function for a desired order and plugging it into the RGE. For example the Adler function to the second order in α_s

$$D(s) = \frac{N_c}{12\pi^2}\left[c_{01} + a_\mu(c_{11} + 2c_{12}L) + a_\mu^2(c_{21} + 2c_{22}L + 3c_{23}L^2)\right], \tag{1.2.12}$$

can be inserted into the eq. 1.2.11

$$4a_\mu c_{12} + 2a_\mu^2(2c_{22} + 6c_{23}L) + \beta_1 a_\mu^2(c_{11} + 2c_{12}L) + \mathcal{O}(a_\mu^3) = 0 \tag{1.2.13}$$

to compare the coefficients order by order in α_s. At order α_μ only the c_{12} term is present and has consequently to be zero. For $\mathcal{O}(a_\mu^2 L)$ solely c_{23} exists as $c_{12} = 0$ and thus also has to vanish. Finally for $\mathcal{O}(a)$ we can relate c_{22} with c_{11} resulting in:

$$c_{12} = 0, \quad c_{22} = \frac{\beta_1 c_{11}}{4} \quad \text{and} \quad c_{23} = 0. \tag{1.2.14}$$

Implementing the newly obtained Adler coefficients we can write out the Adler function to the first order:

$$D(s) = \frac{N_c}{12\pi^2}\left[c_{01} + c_{11}a_\mu\left(c_{21} - \frac{1}{2}\beta_1 c_{11}L\right)a_\mu^2\right] + \mathcal{O}(a_\mu^3). \tag{1.2.15}$$

We have used the RGE to relate Adler function coefficients and thus only need to know coefficients of type $c_{n,1}$. Unfortunately, as we will see in the following section, the RGE gives us two different choices to compute the perturbative contribution to the inclusive τ decay ratio.

Renormalisation group summation

By making use of the RGE we have to decide about the order of mathematical operations we perform. As the all order perturbative contribution δ_{pt} is

independent on the scale μ we are confronted with two choices: *fixed-order perturbation theory* (FOPT) and *contour-improved perturbation theory* (CIPT). Each of them yields a different result, which is the main source of error in extracting the strong coupling from τ decays.

Working in the chiral limit additionally permits us to neglect the longitudinal contribution $D^{(0)}$, in eq. 1.1.11 of the perturbative contribution δ_{pt} of R_τ (eq. 1.2.2). Thus inserting the expansion of $D_V^{(1+0)}$ into the hadronic tau decay width eq. 1.1.11 yields

$$\delta_{pt} = \sum_{n=1}^{\infty} a_\mu^n \sum_{k=1}^{n} k c_{n,k} \frac{1}{2\pi i} \oint_{|x|=1} \frac{dx}{x} (1-x)^3 (1+x) \log\left(\frac{-m_\tau^2 x}{\mu^2}\right)^{k-1}, \tag{1.2.16}$$

where we kept in mind that the contributions from the vector and axial-vector correlator are identical in the massless case.

To continue evaluating the perturbative part we can now either follow the description of FOPT or CIPT. We will now present both.

In FOPT we fix the scale at the tau mass ($\mu^2 = m_\tau^2$), which leaves us with the integration over the logarithm, as seen in

$$\delta_{FOPT}^{(0)} = \sum_{n=1}^{\infty} a(m_\tau^2)^n \sum_{k=1}^{n} k c_{n,k} J_{k-1} \tag{1.2.17}$$

where the contour integrals J_l are defined by

$$J_l \equiv \frac{1}{2\pi i} \oint_{|x|=1} \frac{dx}{x} (1-x)^3 (1+x) \log^l(-x). \tag{1.2.18}$$

The integrals J_l up to order α_s^4 are given by [**Beneke2008**]:

$$J_0 = 1, \quad J_1 = -\frac{19}{12} \quad J_2 = \frac{265}{72} - \frac{1}{3}\pi^2, \quad J_3 = -\frac{3355}{288} + \frac{19}{12}\pi^2. \tag{1.2.19}$$

Using FOPT the strong coupling $a(\mu)$ is fixed at the tau mass scale $a(m_\tau^2)$ and can be taken out of the closed-contour integral. Thus we solely have to integrate over the logarithms $\log(x)$.

Using CIPT, on the contrary, we can sum the logarithms by setting the scale to $\mu^2 = -m_\tau^2 x$ in eq. 1.2.16, resulting in:

$$\delta_{CI}^{(0)} = \sum_{n=1}^{\infty} c_{n,1} J_n^a(m_\tau^2), \tag{1.2.20}$$

where the contour integrals J_l are defined by

$$J_n^a(m_\tau^2) \equiv \frac{1}{2\pi i}\oint_{|x|=1}\frac{dx}{x}(1-x)^3(1+x)a^n(-m_\tau^2 x). \tag{1.2.21}$$

Note that all logarithms vanish, except the ones with index $k = 1$:

$$\log(1)^{k-1} = \begin{cases} 1 & \text{if } k = 1, \\ 0 & k \neq 1 \end{cases} \tag{1.2.22}$$

which selects the Adler function coefficients $c_{n,1}$. Handling the logarithms left us with the integration of the strong coupling $\alpha_s(-m_\tau^2 x)$ over the closed-contour $\oint_{|x|=1}$, which now depends on the integration variable x.

In general we have to decide if we want to perform a contour integration with a constant strong coupling parameter and variable logarithms (FOPT) or "constant logarithms" and a running coupling (CIPT). To emphasise the differences in both approaches we can calculate the perturbative contribution $\delta^{(0)}$ to R_τ for the two different prescriptions yielding [**Beneke2008**]

$$\begin{array}{cccccc} & \alpha_s^2 & \alpha_s^2 & \alpha_s^3 & \alpha_s^4 & \alpha_s^5 \\ \delta^{(0)}_{\text{FOPT}} = & 0.1082 & + 0.0609 & + 0.0334 & + 0.0174 & (+0.0088) = 0.2200(0.2288) \end{array} \tag{1.2.23}$$

$$\delta^{(0)}_{\text{CIPT}} = 0.1479 + 0.0297 + 0.0122 + 0.0086(+0.0038) = 0.1984(0.2021). \tag{1.2.24}$$

The series indicate, that CIPT converges faster and that both series approach a different value. FOPT has larger contributions than CIPT, which leads to a smaller strong coupling if using FOPT. This discrepancy represents currently the biggest theoretical uncertainty for extracting the strong coupling.

As today FOPT or CIPT are equally valid approaches to calculate the perturbative contributions, even though it has been argumented by Beneke et al. [**Beneke2008**] to favour the former. Within this work we will further elaborate the consistency of FOPT and do not state our results in CIPT.

1.2.2 The Non-Perturbative OPE Contributions

The perturbative contribution to the sum rule is the dominant one, but NP have to be taken into account. The contribution of the NP part can be quoted

as [**Jamin2013**]

$$\delta^{NP}_{V+A,FOPT} = -0.086(80), \qquad \delta^{NP}_{V+A,CIPT} = 0.0089(65) \tag{1.2.25}$$

which is small, but not negligible. The NP OPE contributions are commonly categorised by even, increasing dimensions. Contributions of dimension larger than eight are normally neglected, due to the increasing suppression by factors of $1/m_\tau^{2\cdot D}$, where D stands for the corresponding dimension.

The dimension two contributions are proportional to the quark masses and vanish while working in the chiral limit. Consequently we will neglect them and start by stating the $D = 4$ contributions.

1.2.3 Dimension Four

The next apparent OPE contribution is of dimension four. Here we have to take the terms with masses to the fourth power (m^4) into account, the quark condensate multiplied by a mass ($m\langle\overline{q}\,q\rangle$) and the gluon condensate ($\langle GG\rangle$). The resulting expression can be taken from the appendix of [**Pich1999**], yielding:

$$D^{(1+0)}_{ij}(s)\Big|_{D=4} = \frac{1}{s^2}\sum_n \Omega^{(1+0)}(s/\mu^2)a^n, \tag{1.2.26}$$

where

$$\begin{aligned}\Omega^{(1+0)}_n(s/\mu^2) \;=\; & \frac{1}{6}\langle aGG\rangle p^{(1+0)}_n(s/\mu^2) + \sum_k m_k\langle\overline{q}_k q_k\rangle r^{(1+0)}_n(s/\mu^2) \\ & + 2\langle m_i\overline{q}_i q_i + m_j\overline{q}_j q_j\rangle q^{(1+0)}_n(s/\mu^2) \pm \frac{8}{3}\langle m_j\overline{q}_i q_i + m_i\overline{q}_j q_j\rangle t^{(1+0)}_n \\ & - \frac{3}{\pi^2}(m_i^4 + m_j^4)h^{(1+0)}_n(s/\mu^2) \mp \frac{5}{\pi^2}m_i m_j(m_i^2 + m_j^2)k^{(1+0)}_n(s/\mu^2) \\ & + \frac{3}{\pi^2}m_i^2 m_j^2 g^{(1+0)}_n(s/\mu^2) + \sum_k m_k^4 j^{(1+0)}_n(s/\mu^2) + 2\sum_{k\neq l} m_k^2 m_l^2 u^{(1+0)}_n(s/\mu^2)\end{aligned} \tag{1.2.27}$$

The perturbative expansion coefficients are known to second order $\mathcal{O}(a^2)$ for the condensate contributions,

$$\begin{array}{lll} p^{(1+0)}_0 = 0, & p^{(1+0)}_1 = 1, & p^{(1+0)}_2 = \frac{7}{6}, \\ r^{(1+0)}_0 = 0, & r^{(1+0)}_1 = 0, & r^{(1+0)}_2 = -\frac{5}{3} + \frac{8}{3}\zeta_3 - \frac{2}{3}\log(s/\mu^2), \\ q^{(1+0)}_0 = 1, & q^{(1+0)}_1 = -1, & q^{(1+0)}_2 = -\frac{131}{24} + \frac{9}{4}\log(s/\mu^2) \\ t^{(1+0)}_0 = 0 & t^{(1+0)}_1 = 1, & t^{(1+0)}_2 = \frac{17}{2} + \frac{9}{2}\log(s/\mu^2). \end{array} \tag{1.2.28}$$

while the m^4 terms have been only computed to first order $\mathcal{O}(a)$

$$\begin{aligned}
h_0^{(1+0)} &= 1 - 1/2\log(s/\mu^2), & h_1^{(1+0)} &= \tfrac{25}{4} - 2\zeta_3 - \tfrac{25}{6}\log(s/\mu^2) - 2\log(s/\mu^2)^2,\\
k_0^{(1+0)} &= 0, & k_1^{(1+0)} &= 1 - \tfrac{2}{5}\log(s/\mu^2),\\
g_0^{(1+0)} &= 1, & g_1^{(1+0)} &= \tfrac{94}{9} - \tfrac{4}{3}\zeta_3 - 4\log(s/\mu^2),\\
j_0^{(1+0)} &= 0, & j_1^{(1+0)} &= 0,\\
u_0^{(1+0)} &= 0, & u_1^{(1+0)} &= 0.
\end{aligned} \tag{1.2.29}$$

The above condensates all depend on the scale μ^2, but we can express them in form of the scale-invariant gluon-and quark-condensate [**Spiridonov1988**], which are combinations of the minimally subtracted operators

$$\begin{aligned}
\beta_1\langle aG^2\rangle_I \equiv \beta(s)\langle G^{\mu\nu}_{(a)}G^{(a)}_{\mu\nu}\rangle + 4\gamma(a)\sum_{i=u,d}\langle m_i\overline{q}_i q_i\rangle \\
- \frac{3}{4\pi^2}\sum_{i,j=u,d} m_i^2 m_j^2 \gamma_0^{ij}(a)
\end{aligned} \tag{1.2.30}$$

$$\langle m_i\overline{q}_j q_j\rangle \equiv \langle\overline{q}_j q_j\rangle + \frac{3m_i m_j^3}{7\pi^2 a}\left\{1 - \frac{53}{24}a + \mathcal{O}(a^2)\right\}, \tag{1.2.31}$$

where $\gamma_0^{ij}(a) = -2 - 8/3a$. During this work we will insert the known invariant quark condensates (see **??**) as constants and state our results for the invariant gluon condensate.

1.2.4 Dimension Six and Eight

Our application of dimension six contributions is founded in [**Braaten1991**] and has previously been calculated beyond leading order by [**Lanin1986**]. The operators appearing are the masses to the power six (m^6), the four-quark condensates ($\langle\overline{q}\,q\overline{q}\,q\rangle$), the three-gluon condensates ($\langle g^3G^3\rangle$) and lower dimensional condensates multiplied by the corresponding masses, such that in total the mass dimension of the operator will be six. The largest contributions comes from the 4-quark operators. The three-gluon condensate does not contribute at leading order [**Hubschmid1982**] and is neglected. Operators proportional to the light quark masses will also be neglected. The resulting contribution of dimension six operators has been calculated in [**Lanin1986**] and leads to a large amount of operators, which until today cannot be accurately determined by phenomenology methods. To reduce the number of operators we can

make use of the *vacuum saturation approach* (VSA) [**Beneke2008**, **Braaten1991**, **Shifman1978**] to express them in quark condensates $\langle q\overline{q}\rangle$. For Wilson coefficients of order α_s and applying the vacuum saturation we get a dimension six contributions of

$$D^{1+0}_{ij,V/A}(s)\Big|_{D=6} = \frac{32\pi^2}{3}a(\mu)\frac{\langle\overline{q}_i q_i(\mu)\rangle\langle\overline{q}_j q_j\rangle}{s^3} - \frac{32}{7}\pi^2 a_\mu \frac{\langle\overline{q}_i q_i\rangle^2\langle\overline{q}_j q_j\rangle^2}{s^3}. \quad (1.2.32)$$

Unfortunately the scaling properties of the dimension six contribution, resulting from the VSA, are inconsistent with the scaling properties of the 4-quark operators [**Narison1983**, **Jamin1985**] and terms of order α_s^2 are usually ignored. In addition to the scaling problematic the VSA is known to underestimate the dimension six contribution [**Launer1983**].

In our work we take the simplest approach possible: Introducing an effective dimension six coefficient $\rho^{(6)}_{V/A}$ divided by the appropriate power in s

$$D^{(1+0)}_{ij,V/A}(s)\Big|_{D=6} = 3\frac{\rho^{(6)}_{V/A}}{s^3}. \quad (1.2.33)$$

Here we also neglected the scale dependence of the dimension six operator, which is determined by the anomalous dimension. We have calculated the leading-order anomalous dimension matrices corresponding to the dimension-6 four-quark operators of flavour non-diagonal, as well as flavour diagonal, mesonic vector and axial-vector currents in [**Boito2015**].

As for the dimension eight contribution the situation is not better than the dimension six one we keep the simplest approach, leading to

$$D^{(1+0)}_{ij,V/A}\Big|_{D=8} = 4\frac{\rho^{(8)}_{V/A}}{s^4}. \quad (1.2.34)$$

The NP contribution of dimension eight is the highest order that we are going to implement. Higher orders will be neglected. Next to the NP treatment of the OPE we have to discuss possible DV.

1.3 Duality Violations

As seen in **??** we have to assume quark-hadron duality for the QCDSR to work. Unfortunately duality is always to some extend broken through so-called DV,

which are well known [**Cata2008**, **Cata2009**]. Experimental data show an oscillating behaviour that cannot be reproduced by the OPE. Moreover in the large N_c limit it can be shown that DV have an exponential decreasing, sinusoidal appearance [**Cata2005**]. Consequently for the cases with apparent DV we have to somehow include the corrections coming from DV and adapt eq. 1.2.2, leading to

$$R^{\omega}_{\tau,V/A} = \frac{N_c}{2} S_{EW} |V_{ud}|^2 \left(1 + \delta^{\omega}_{pt} + \delta^{\omega}_{npt} + \delta^{\omega}_{dv}\right), \tag{1.3.1}$$

where we extracted δ_{dv} from δ_{npt}, even though DV are NP. The DV correction has been modelled with the following ansatz [**Cata2009**]

$$\rho^{DV}_{V/A}(s) = e^{-(\delta_{V/A} + \gamma_{V/A} s)} \sin(\alpha_{V/A} + \beta_{V/A} s), \tag{1.3.2}$$

which contains four parameters for the vector and another four parameters for the axial-vector contribution. Note that for fitting the kinematic weight in the V-channel, which is known to be sensible for DV at lower energies [**Boito2011a**], we would have seven parameters instead of only three. Making use of the model (eq. 1.3.2) the DV then appear as an additional term in the inclusive tau decay ratio

$$R_{\tau,V/A} = -\pi i \oint_{|s|=m_\tau^2} \frac{dx}{x}(1-x)^3 \left[3(1+x)D^{(1+0)}(m_\tau^2 x) + 4D^{(0)}(m_\tau^2 x)\right] + \mathcal{D}_{V/A}(m_\tau^2), \tag{1.3.3}$$

where the DV contributions would be given as

$$\mathcal{D}_{\omega}(m_\tau^2) = -12\pi^2 \int_{m_\tau^2}^{\infty} \frac{ds}{m_\tau^2} \omega(s) \rho_{V/A}. \tag{1.3.4}$$

1.3.1 Pinched Weights to avoid DVs

The general QCDSR (**??**) contain a weight function ω, which is not only used to suppress higher order dimensions, but also DV. The weights that suppress DV are so-called pinched weights of the form

$$\omega(s) = \left(1 - \frac{s}{m_\tau^2}\right)^k, \tag{1.3.5}$$

where k is the degree of the pinched weight. The higher the degree of the pinching, the lower the contribution of the critical region close to the real axis

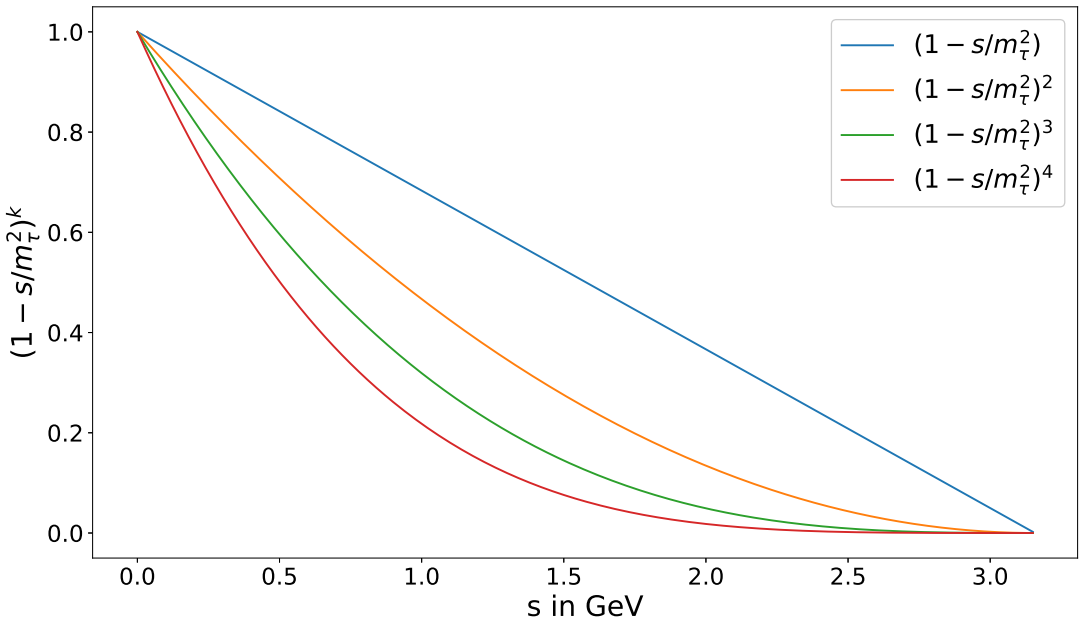

Figure 1.2: Pinched weights $(1 - s/m_\tau^2)^k$ for degrees 1 to 4. We can see that weights of higher pinching decrease faster, which comes in handy if we want to suppress duality violations.

(see. fig. 1.2). Thus for higher pinchings we are better protected from DV effects. For the transversal component of the inclusive τ decay ratio (eq. 1.1.2) a pinching of second degree appears quite naturally as the kinematic weight (see **??**). In general it is said that a double pinched weight is sufficient to neglect effects caused by DV. In our analysis we show that double pinched weights indeed sufficiently suppress DV and that even single pinched weights yield acceptable results. Additionally to applying pinched weights we focus on combinations of vector and axial-vector contributions, which as we will see, regarding the ALEPH data have visibly suppressed DV.

1.4 Borel Summation

The Adler function of eq. 1.1.5 is given by a divergent asymptotic series. We only know the needed Adler function coefficients $c_{n,m}$ up to fifth order. To get the best possible sum for such a series we can apply the *Borel summation* (BS). The BS is an long known summation method for divergent series introduced

by Émile Borel [**Emile1899**].

Regarding the sum

$$A = \sum_{n=0}^{\infty} a_k \tag{1.4.1}$$

we can introduce the faculty of n, which can be rewritten in its integral form

$$A = \sum_{n=0}^{\infty} \frac{n!}{n!} a_k = \sum_{n=0}^{\infty} \frac{a_k}{n!} \int_0^{\infty} e^{-t} t^n \, dt. \tag{1.4.2}$$

Interchanging the integral and the sum is referred to as the Borel integral

$$A \equiv \int_0^{\infty} dt e^{-t} \sum_{n=0}^{\infty} \frac{a_k}{n!} t^n, \tag{1.4.3}$$

which contains the Borel transform

$$B[A](t) = \sum_{n=0}^{\infty} \frac{a_k}{n!} t^n. \tag{1.4.4}$$

The Borel integral is only valid for Borel transforms with no singularities for real positive t. In the cases of a valid Borel integral the BS can now be used to get exact answers of divergent series, by first applying the Borel transform and then integrating over it with the help of the Borel integral.

In our case we want to calculate the BS of the Adler function given in eq. 1.1.5 to argue if FOPT or CIPT gives the better approximation to the τ decay ratio. For convenience the Adler function is redefined as

$$\frac{12\pi^2}{N_c} D_V^{1+0}(s) \equiv 1 + \widehat{D}(s) \equiv 1 + \sum_{n=0}^{\infty} r_n \alpha_s(\sqrt{(s)})^{n+1}. \tag{1.4.5}$$

Then we apply the Borel transformation to $\widetilde{D}$

$$B[\widehat{D}](t) \equiv \sum_{n=0}^{\infty} r_n \frac{t^n}{n!} \quad \text{with} \quad t \in C. \tag{1.4.6}$$

As t is in general a complex number we can study the Borel transform in the so-called Borel plane. The Borel plane for the Adler function is visualised in fig. 1.3. For real t the Borel transform of the Adler function has poles. Poles of the Borel transform are referred to as renormalons [**Beneke1999**, **Zichichi1979**]. We have to distinguish between *ultraviolet* (UV) and *infrared*

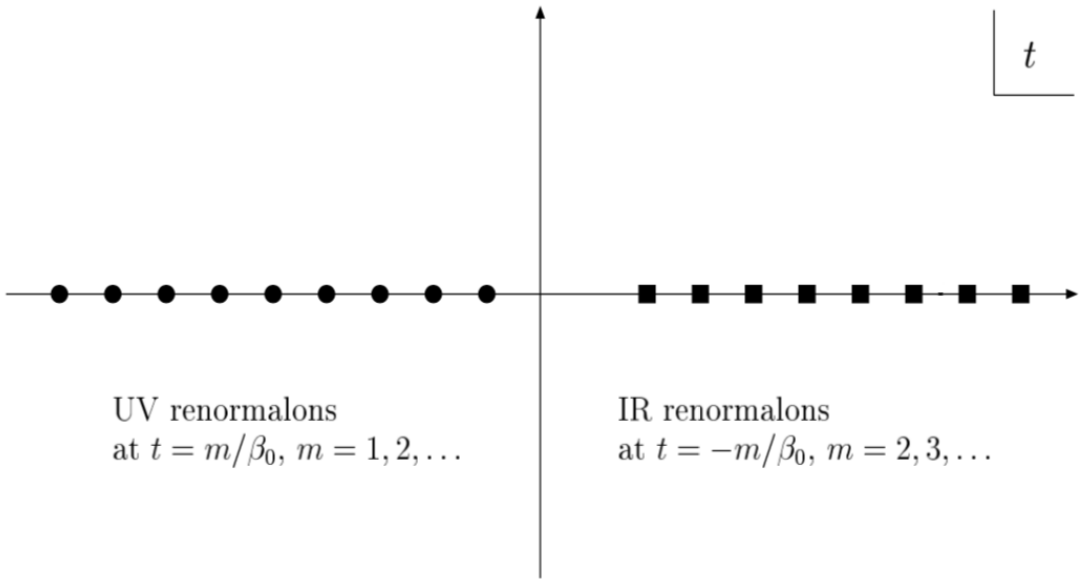

Figure 1.3: Singularities in the Borel plane of the Adler function, taken from[**Beneke1998**].

(IR) renormalons. UV renormalons are located at $t = m/\beta_0$ with positive integer $m = 1, 2, \ldots$ and IR renormalons are located at $t = -m\beta_0$ with positive integer $m = 2, 3, \ldots$. Due to the poles of the positive real axis the Borel interal

$$\widehat{D}(\alpha) \equiv \int_0^\infty dt e^{-t/\alpha} B[\widehat{D}](t) \tag{1.4.7}$$

is not well defined. Consequently to have a valid Borel integral we have to move the contour above or below the singularities.

The ansatz we use to express the Adler function in terms of the Borel sum was introduced by Beneke et al. [**Beneke2008**]. They have build a physical model for the Adler function series

$$B[\widehat{D}](u) = B[\widehat{D}_1^{UV}](u) + B[\widehat{D}_2^{IR}](u) + B[\widehat{D}_3^{IR}](u) + d_0^{PO} + d_1^{PO} u, \tag{1.4.8}$$

where $B[\widehat{D}_p^{UV/IR}](u)$ are ansätze for the ultraviolet and infrared appearing renormalon poles

$$B[\widehat{D}_p^{IR}](u) \equiv \frac{d_p^{IR}}{(p-u)^{1+\tilde{\gamma}}} \left[1 + \tilde{b}_1(p-u) + \tilde{b}_2(p-u)^2 + \ldots\right] \tag{1.4.9}$$

$$B[\widehat{D}_p^{UV}](u) \equiv \frac{d_p^{UV}}{(p+u)^{1+\tilde{\gamma}}} \left[1 + \bar{b}_1(p+u) + \bar{b}_2(p+u)^2\right], \tag{1.4.10}$$

which have been defined in section five of [**Beneke2008**]. As the large order behaviour of the Adler function is governed by a sign-alternating UV renormalon divergence and the lower-orders are not, only the leading UV singularity has been included. Furthermore the intermediate orders are governed by IR renormalons. Thus the first two ($m = 2$ and $m = 3$) have been included into the model. The five parameters d_1^{UV}, d_2^{IR}, d_3^{IR}, d_0^{PO} and d_1^{PO} have then to be matched to the known perturbative expansion of the Adler function. They are found to be [**Beneke2008**]

$$\begin{aligned} d_1^{UV} = -0.0156, \quad d_2^{IR} = 3.16, \quad d_3^{IR} = -13.5, \\ d_0^{PO} = 0.781 \quad \text{and} \quad d_1^{PO} = 0.00766. \end{aligned} \tag{1.4.11}$$

We will apply the Borel integral of this model to perform fits as an alternative to FOPT for the experimental data we are going to describe in the upcoming section.

1.5 Experiment

The τ decay data we use to perform our QCD analysis is from the ALEPH experiment. The ALEPH experiment was located at the *large-electron-positron* (LEP) collider at *European Organisation for Nuclear Research* (CERN) in Geneva. LEP started producing particles in 1989 and was replaced in the late 90s by the *large-hadron-collider* (LHC), which makes use of the same tunnel of 27 km circumference. The data produced within the experiment is still maintained by former ALEPH group members led by M. Davier, which have performed regular updates on the data-sets [**Davier2013**, **Davier2008**, **Aleph2005**]. The last update was motivated by Boito et al. [**Boito2010**], who discovered irregularities in the covariances by comparing data from a Monte Carlo generator with the ALEPH.

The measured spectral functions for the ALEPH data are defined in [**Davier2007**]

and given for the transverse and longitudinal components separately

$$\begin{aligned}\rho^{(1)}_{V/A}(s) = \frac{m_\tau^2}{12|V_{ud}|^2 S_{EW}} \frac{\mathcal{B}(\tau^- \to V^-/A^- \nu_\tau)}{\mathcal{B}(\tau^- \to e^- \overline{\nu}_e \nu_\tau)} \\ \times \frac{dN_{V/A}}{N_{V/A}\, ds} \left[\left(1 - \frac{s}{m_\tau^2}\right)^2 \left(1 + \frac{2s}{m_\tau^2}\right)\right]^{-1} \\ \rho^{(0)}_{A}(s) = \frac{m_\tau^2}{12|V_{ud}|^2 S_{EW}} \frac{\mathcal{B}(\tau^- \to \pi^-(K^-)\nu_\tau)}{\mathcal{B}(\tau^- \to e^- \overline{\nu}_e \nu_\tau)} \times \frac{dN_A}{N_A\, ds} \left(1 - \frac{s}{m_\tau^2}\right)^{-2}.\end{aligned} \tag{1.5.1}$$

The data relies on a separation into vector and axial-vector channels. In the case of the π this can be achieved via counting. The vector channel is characterised by a negative G-parity, whereas the axial-vector channel has positive G-parity. A single π carries negative G-parity, an even number of π carries positive G-parity and an odd number of π carries negative G-parity:

$$n \times \pi = \begin{cases} \text{vector} & \text{if } n \text{ is even,} \\ \text{axial-vector} & \text{otherwise.} \end{cases} \tag{1.5.2}$$

The separation into vector and axial-vector channel of mesons including strange quarks, like $K\overline{K}$ pairs, is more difficult, because these are not in general eigenstates of G-parity and contribute to both V and A channels.

The contributions to the spectral function for the vector, axial-vector and V+A channel can be seen in fig. 1.4. The dominant modes in the vector case are **[Davier2006]** decays into two ($\tau^- \to \pi^-\pi^0\nu_\tau$) or four ($\tau^- \to \pi^-\pi^-\pi^+\pi^0\nu_\tau$) pions. The first of these is produced by an intermediate $\rho(770)$ meson, which in contrary to the pions carries angular momentum of one and is clearly visible as peak around 770 GeV in fig. 1.4a. The dominant modes in the axial-vector case are decays into one ($\tau^- \to \pi^-\nu_\tau$) or three ($\tau^- \to \pi^-\pi^0\pi^0\nu_\tau$ and $\tau^- \to \pi^-\pi^-\pi^+\nu_\tau$) pions. Here the three pion final states stem from the a_1^--meson, which can be seen as a peak in fig. 1.4b.

We furthermore added the perturbative contribution for a fixed $\alpha_s(m_\tau) = 0.329$ using FOPT in fig. 1.4c. We can see, that the perturbative contribution (the blue line) is an almost straight line and cannot reproduce the oscillating behaviour, given by the ALEPH data. This is especially the case for the V and A channel and is seen as an indicator for DV. Even including NP, higher dimensions of

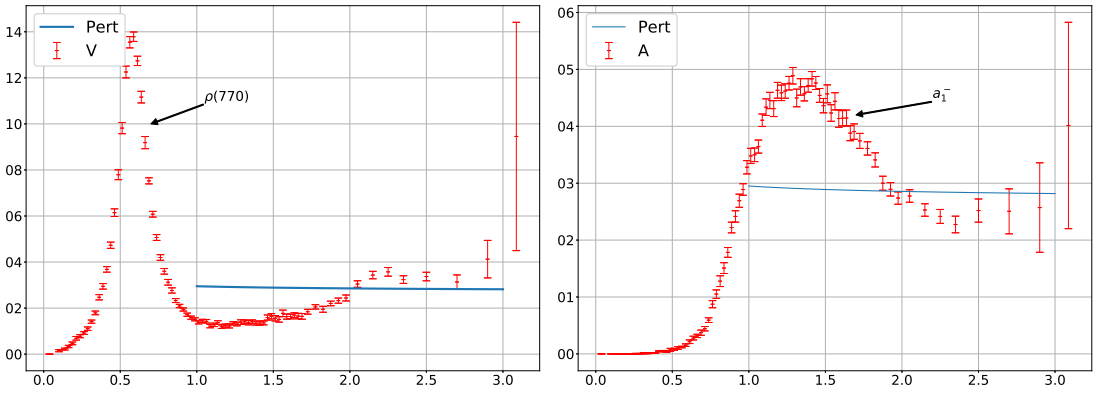

(a) Vector (b) Axial-Vector

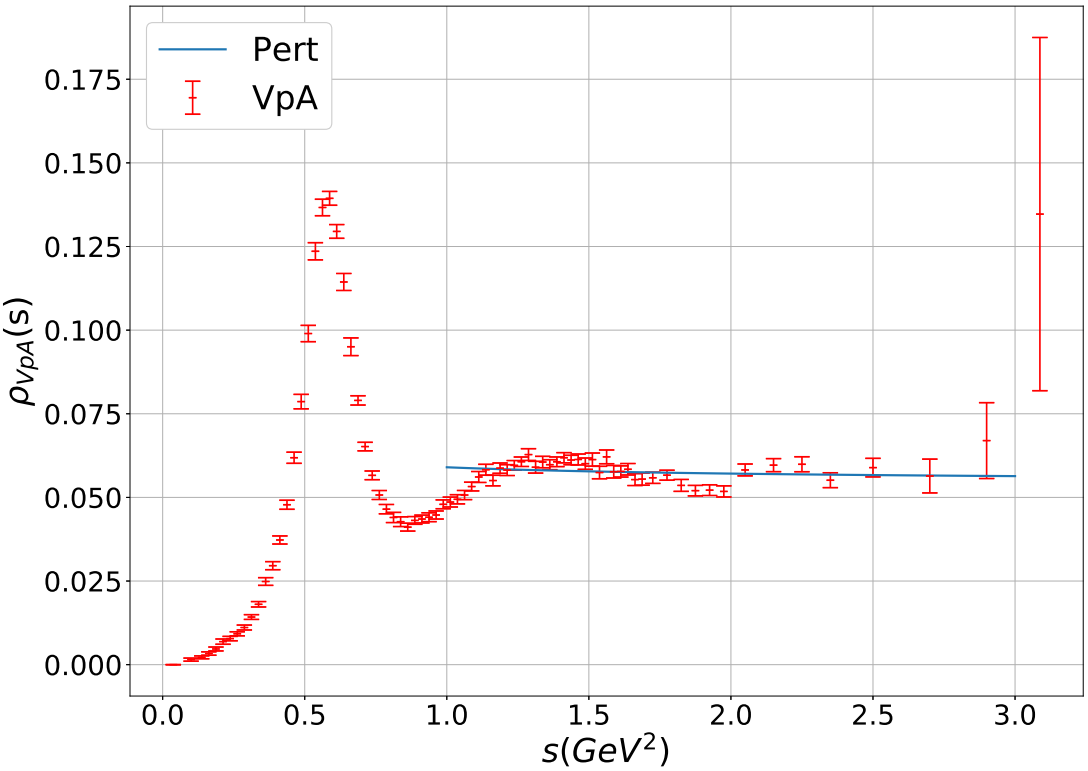

(c) Vector plus Axial-Vector

Figure 1.4: Visualisation of the vector, axial-vector and V+A spectral function given by the ALEPH data [**Davier2013**] in red with errors. We also plotted the FOPT theoretical calculation up to third order in α_s, for a fixed $\alpha_s(\tau) = 0.329$ in blue. Note that the perturbative contribution can only limited represent the experimental data. It does not reproduce the sinusoidal form.

the OPE is not reproducing the wavy structure. In the case of V+A, we have an higher agreement between our perturbative graph and the data. In general we believe that DV are sufficiently suppressed in the case of V+A and will argument in favour of this statement in the following chapter. This is only the case for energies larger than 1.5 GeV, as the ρ resonance of the V channel is impossible to be represented by perturbative tools. For lower energies DV become too important to be neglected.

1.5.1 Total decay ratio from experimental data

The data has been last revised in 2014 [**Davier2013**] and is publicly available [**AlephData**]. It consists of the mass squared bin center (*sbin*), the bin size (*dsbin*), the normalised invariant mass squared distribution (*sfm2*), the total errors (*derr*) and their correlations (*corerr*). To make the data comparable to our theoretical calculations we have to give the normalised invariant mass squared distribution (*sfm2*) in form of the total decay ratio R_τ. The data is given as the normalised invariant mass squared distribution $(dN_i/ds)/N_i$ scaled by a factor 100 and further normalised to the corresponding branching ratio $i \in \{V,A,V+A\}$. Thus we can connect the branching ratio of the i-channel to *sfm2* as follows

$$\mathcal{B}_{V/A} \equiv \int_0^{s_\tau} ds \frac{sfm2_{V/A}(s)}{100} \equiv \int_0^{s_\tau} ds \mathcal{B}_{V/A} \left(\frac{dN_{V/A}}{N_{V/A}\, ds} \right), \tag{1.5.3}$$

where we used $s_\tau \equiv m_\tau^2$. The total decay ratio R_τ is defined as the decay width of τ decaying into hadrons over τ decaying into electrons. It and can be expressed via the corresponding branching ratios, which can be connected to the invariant mass squared distribution sfm2

$$R_{\tau,V/A} = \frac{\mathcal{B}_{V/A}}{\mathcal{B}_e} = \int_0^{s_\tau} ds \frac{sfm2_{V/A}(s)}{100\mathcal{B}_e}. \tag{1.5.4}$$

Theoretically the decay ratio is given in eq. 1.0.1. If we neglect the longitudinal contribution $\mathrm{Im}\,\Pi^{(0)}(s)$ and remember the definition of the spectral function (**??**) and the kinematic weight (**??**), we can write the decay ratio as

$$R_{\tau,i} = \int_0^{s_\tau} \frac{ds}{s_\tau} \omega_\tau(s) \rho(s) \tag{1.5.5}$$

and thus relate the spectral function to the experimental data

$$\rho(s) = \frac{s_\tau}{12\pi^2 100\mathcal{B}_e}\frac{\text{sfm2}}{\omega_\tau}. \tag{1.5.6}$$

To fit the experimental data we define a so-called *spectral function moment* (or *moment*)

$$I_i^{\text{exp},\omega} \equiv \int_0^{s_0}\frac{ds}{s_0}\omega\left(\frac{s}{s_0}\right)\rho(s), \tag{1.5.7}$$

which will be used in our χ^2 fits, explained in the upcoming section. The data is given for discrete bins so we have to express the integral of the spectral function moment as sum over those bins. The final expression we use to fit parameters to the experimental data is then given by

$$I^{\omega}_{\text{exp},V/A}(s_0) = \frac{s_\tau}{100\mathcal{B}_e s_0}\sum_{i=1}^{N(s_0)}\frac{\omega\left(\frac{s_i}{s_0}\right)}{\omega_\tau\left(\frac{s_i}{s_\tau}\right)}\,\text{sfm2}_{V/A}(s_i). \tag{1.5.8}$$

1.6 The Method of Least Squares

We apply *method of least squares* (LS) to fit the parameters $\vec{\alpha}$ from the experimental data. Our χ^2-function can be expressed as

$$\chi^2 = \left(I_i^{\text{exp}} - I_i^{\text{th}}(\vec{\alpha})\right) C_{ij}^{\text{exp}-1}\left(I_j^{\text{exp}} - I_j^{\text{th}}(\vec{\alpha})\right), \tag{1.6.1}$$

where $I^{\text{exp}}/I^{\text{th}}$ is a vector of experimental moments/ theoretical moments with the same weight, but different energy cutoffs s_0, labelled by the index i. In addition C^{exp} is the covariance matrix describing the correlation of the different experimental moments $C_{ij}^{\text{exp}} = \text{cov}[I_i^{\text{exp}} I_j^{\text{exp}}]$, which can be computed by the given correlation matrix of the ALEPH data.

In general we aim to minimise the value of χ^2, which will fix the parameter vector $\vec{\alpha}$. The properties of the χ^2-function are well known and the best fits are characterised through $\chi^2/\text{dof} \approx 1$, where the DOF of the fit can be calculated through

$$\text{DOF} = \text{experimental moments} - \text{parameters}. \tag{1.6.2}$$

E.g. if we want to fit α_s and the dimension four Wilson coefficient C_4 we get $7 - 2 = 5$ DOF.

For our purposes we use the numerical minimisation computer program MINUIT, which was originally written in FORTRAN by Fred James in the 1970 [**James1975**]. Today in its second version the program has been ported to C++ by the ROOT [**Brun1997**] project at CERN.

The parameter vector $\vec{\alpha}$ includes the strong coupling α_s, but also the included OPE Wilson coefficient. Consequently we should have at least as many, if not more moments as parameters we want to fit. As the moments for different s_0 are highly correlated we are limited to fit a set of only a few parameters.

It is also possible to increase the number of moments used by applying multiple weights ω. Unfortunately using different weights leads to highly correlated moments, which cause numerical complications by inverting the covariance matrix in eq. 1.6.1. To handle the high correlations we have to redefine our fit quality.

1.6.1 Block Diagonal "Fit-Quality"

For fits including multiple weights, which we do not perform in this work, we can redefine LS [**Boito2014**] to

$$Q^2 = \sum_{\omega} \sum_{s_0^i, s_0^j} \left(I_\omega^{exp}(s_0^i) - I_\omega^{th}(s_0^i, \vec{\alpha}) \right) \widetilde{C}^{-1}_{ij,\omega} \left(I_\omega^{exp}(s_0^j) - I_\omega^{th}(s_0^j, \vec{\alpha}) \right), \tag{1.6.3}$$

where the covariance matrix $\widetilde{C}$ is now a diagonal of the experimental covariance matrices C_ω^{exp} for each weight

$$\widetilde{C} = \begin{pmatrix} C^{exp}_{\omega=1} & 0 & \dots & 0 \\ 0 & C^{exp}_{\omega=2} & \ddots & \vdots \\ \vdots & \ddots & \ddots & 0 \\ 0 & \dots & 0 & C^{exp}_{\omega=n} \end{pmatrix}. \tag{1.6.4}$$

As a result we are still able to invert the newly defined covariance matrix $\widetilde{C}$, but minimisation routines like CERN MINUIT are not able to calculate the proper errors for the parameters we want to extract. We have to perform our own error propagation to obtain meaningful errors for the parameters. The error

propagation has been derived in [**Boito2011a**, **Boito2011**] and is given as

$$\langle \delta\alpha_k \alpha_l \rangle = A^{-1}_{km} A^{-1}_{ln} \frac{\partial I^{th}_i(\vec{\alpha})}{\partial \alpha_m} \frac{\partial I^{th}_r(\vec{\alpha})}{\partial \alpha_n} \widetilde{C}^{-1}_{ij} \widetilde{C}^{-1}_{ij} \langle \delta I^{exp}_k \delta I^{exp}_l \rangle, \tag{1.6.5}$$

where

$$A_{kl} = \frac{\partial I^{th}(\vec{\alpha})}{\partial \alpha_k} C^{-1}_{ij} \frac{I^{th}_j(\vec{\alpha})}{\alpha_l}. \tag{1.6.6}$$